Virus Research

Characterisation of different forms of the accessory gp3 canine coronavirus type I protein identified in cats

Anne-Laure Pham-Hung d'Alexandry d'Orengiani [a,b,c], Lidia Duarte [a,b,c], Nicole Pavio [a,b,c], Sophie Le Poder [a,b,c,*]

[a] Université Paris-Est, Ecole Nationale Vétérinaire d'Alfort, UMR 1161 Virology, Maisons-Alfort, France
[b] INRA, UMR 1161 Virology, Maisons-Alfort, France
[c] ANSES, Animal Health Laboratory, UMR 1161 Virology, Maisons-Alfort, France

ARTICLE INFO

ABSTRACT

ORF3 is a supplemental open reading frame coding for an accessory glycoprotein gp3 of unknown function, only present in genotype I canine strain (CCoV-I) and some atypical feline FCoV strains. In these latter hosts, the ORF3 gene systematically displays one or two identical deletions leading to the synthesis of truncated proteins gp3-Δ1 and gp3-Δ2. As deletions in CoV accessory proteins have already been involved in tissue or host switch, studies of these different gp3 proteins were conducted in canine and feline cell. All proteins oligomerise through covalent bonds, are N-glycosylated and are maintained in the ER in non-infected but also in CCoV-II infected cells, without any specific retention signal. However, deletions influence their level of expression. In canine cells, all proteins are expressed with similar level whereas in feline cells, the expression of gp3-Δ1 is higher than the two other forms of gp3. None of the gp3 proteins modulate the viral replication cycle of heterologous genotype II CCoV in canine cell line, leading to the conclusion that the gp3 proteins are probably advantageous only for CCoV-I and atypical FCoV strains.

1. Introduction

The genome of the *Coronaviridae* (CoV) family is a large single-stranded and positive-sense RNA molecule of about 30 kDa (Gorbalenya et al., 2006). For all CoVs, the first two thirds of the genome encode non-structural proteins which are essentially involved in the CoV replication and transcription machinery (Bredenbeek et al., 1990). The rest of the genome comprises genes of the structural proteins S (spike), E (envelope), M (membrane), N (nucleocapsid) and eventually HE (hemagglutinin–esterase) (De Groot, 2006). Additional genes named accessory genes are interspaced between genes encoding the structural proteins. The number and position of these genes vary from one CoV to another. With eight accessory genes, SARS-CoV possesses the highest number of them, whereas hCoV-229E contains only one (Dijkman et al., 2006).

Feline CoV (FCoV) and canine CoV (CCoV) are common pathogens of cat and dog populations, sometimes leading to fatal diseases (Pedersen, 2009; Decaro and Buonavoglia, 2008). CCoVs are separated into two genetic clusters, CCoV-I and CCoV-II, according to the S gene sequence. One accessory gene, named ORF3 is a singularity of the CCoV genotype I (CCoV-I). Its sequence is highly conserved among CCoV-I, suggesting its importance in some aspects of the viral infection. It is the only CCoV accessory gene which has been investigated so far. *In vitro* translation assays demonstrated that ORF3 encodes an N-glycosylated protein of 28 kDa, named gp3 (Lorusso et al., 2008). Still, the function of gp3 remains unknown. Our recent phylogenetic studies conducted on the characterisation of CoV strains infecting cats lead to the discovery of atypical FCoV strains harbouring a feline S gene and downstream genes genetically related to CCoV-I. Sequences of the ORF3 gene were also present in these strains but displayed deletions never described so far. All ORF3 sequences from atypical FCoV strains shared a deletion of 29-nt, which introduced a stop codon and another frequently observed deletion of 27-nt deleted the predicted protein of nine additional a.a. (Le Poder et al., 2013). The complete gp3 protein of CCoV-I is of 207 a.a. in length, whereas the deleted forms present in atypical FCoV strains are predicted to produce either a deleted protein, named gp3-Δ1 of 158 a.a. or another form, named gp3-Δ2, of 149 a.a. In comparison with gp3, gp3-Δ1 and gp3-Δ2 lost the C-terminus part from the cysteine residue in position 157 onward. Gp3-Δ2 is further truncated of 9 a.a. between

* Corresponding author at: Université Paris-Est, Ecole Nationale Vétérinaire d'Alfort, UMR 1161 Virology, 94704 Maisons-Alfort, France.
Tel.: +33 1 43 96 73 25; fax: +33 1 43 96 73 96.
E-mail address: slepoder@vet-alfort.fr (S. Le Poder).

Lys[88] and Phe[96]. All proteins maintain a predicted signal peptide at the N-terminus extremity and a putative glycosylation site on Asn[116]. No other particular functional domain was predicted by *in silico* analysis.

Coronaviruses are well known for crossing the species barrier, sometimes leading to the emergence of new pathogens, like the SARS-CoV or the MERS-CoV. Adaptation to a new host is often accompanied by modifications of some accessory proteins, among others (McBride and Fielding, 2012). With the aim of understanding the role of the gp3 deletions in the adaptation of atypical FCoVs to the feline species, we characterised the basic properties of the different forms of gp3 in both feline and canine cells. The absence of culture-cell adapted strains of CCoV-I and of the newly discovered atypical FCoV strains impaired studies of the different gp3 proteins in cells culture infected with these specific CoVs. Through transient transfection of plasmids expressing the different proteins, we demonstrated that the gp3 deletions influence their expression. The complete gp3 protein is expressed only in canine cells, gp3-Δ1 is expressed at a high level in both canine and feline cells and gp3-Δ2 is faintly observed in feline cell lines. In contrast, all proteins assemble into covalent oligomers and are maintained in the endoplasmic reticulum (ER) despite cleavage of their peptide signal and absence of a known specific retention signal. In canine transfected cells and infected by CCoV-II, which does not harbour the ORF3 gene, the gp3 proteins are also localised in the ER but none influence the viral production of CCoV-II strains.

2. Materials and methods

2.1. Cell culture and transient transfection

Canine A72 and feline CrFK cells were maintained in Dulbecco's modified Eagle's medium (DMEM) (Invitrogen, Life Technologies) supplemented with 10% foetal bovine serum, 1% penicillin–streptomycin solution, 1% sodium-pyruvate and 1% non-essential amino acids.

Subconfluent A72 and CrFK cells were transfected in 6-well plates with 2.5 μg DNA plasmid using TransIT-LTI transfection reagent (Mirus), following the manufacturer's instructions.

2.2. Plasmids

Optimised codon sequences of the complete ORF3 gene (GenBank accession numbers JN714200), and the two deleted gene forms (GenBank accession numbers JN714196 and JN714199) were synthesised in frame with the 3xFlag tag into pCDNA3.1 plasmids (Invitrogen) between restriction site BamHI and NotI, by Proteogenix (ProteoGenix SAS, France).

Mutant plasmids with deletion of the signal peptide of the ORF3 genes were subsequently generated from each parental plasmid. Briefly, plasmids consisting of residues 15 to the stop codon, were obtained by PCR assays with the forward primers (ΔSP-ORF3 F1: 5′-GGACTAGTGGATCCATGCACCCCTTTCACG-3′, ΔSP-ORF3-Δ1/Δ2 F1: 5′-TCCGCCGCCACCATGCTCCACCCCTTTCAC-3′) and reverse primers (ΔSP-ORF3 R1: 5′-CGTGAAAGGGGTGCATGGATCCACTAG-TCC-3′, ΔSP-ORF-Δ1/Δ2 R1: 5′-GTGAAAGGGGTGGAGCATGGTGG-CGGCGGA-3′). To create gp3 proteins with uncleaved signal sequence, the amino acids critical for cleavage were changed into five Leucine residues by PCR assays using the following primers (5L-ORF3 F2: 5′-ATCAGTGTCGTCCTTTTGTTATTACTCCACCCCTTT-3′, 5L-ORF3 R2: 5′-AAAGGGGTGGAGTAATAACAAAAGAAGGACACT-GAT-3′, 5L-ORF3-Δ1/Δ2 F2: 5′-ATGATTAGTGTGGTCCTTTTGTTAT-TACACCCCTTTCAC-3′, 5L-ORF3-Δ1/Δ2 R2: 5′-CGTGAAAGGGG-TGTAATAACAAAAGGACCACACTAAT CAT-3′). PCR products were submitted to digestion by DpnI enzyme (New England Biolabs) during 1 h at 37 °C to eliminate the parental plasmid. Library Efficiency DH5α bacteria (Invitrogen) were transformed with the digestion products according to the manufacturer's recommendations.

2.3. Immunoblotting

At 24 h post-transfection, cells were lysed with RIPA extraction buffer (20 mM Tris–HCl, pH 7.5, 0.2% Nonidet P-40, 150 mM NaCl, 0.5 mM EGTA, 1.5 mM MgCl$_2$, 10% Glycerol) supplemented with Complete Protease Inhibitor Cocktail Tablet (Roche). Samples containing 100 μg of total proteins were then mixed with an equal volume of 5× Laemmli buffer and heated at 95 °C for 5 min. Where mentioned, 10% of β-mercaptoethanol was added to cell lysates. Proteins were separated on sodium dodecyl sulphate (SDS)-polyacrylamide gel electrophoresis (PAGE) and transferred onto a nitrocellulose membrane (GE Healthcare). After saturation with 5% milk in PBS–Tween (0.01%) buffer (PBST), the membranes were incubated with anti-Flag monoclonal antibody (Sigma–Aldrich) diluted at 1/5000 or anti-actin monoclonal antibody (Sigma–Aldrich) diluted at 1/2000 in PBST–milk buffer overnight at 4 °C. The membranes were washed three times in PBST buffer and incubated for 1 h at room temperature with horseradish peroxidise-conjugated anti-mouse antibody (Roche) diluted at 1/5000 in PBST-milk buffer. After three washes, blots were revealed using enhanced chemiluminescence (ECL) reagents (Pierce) and analysed with a Fusion imaging system (Bio-Rad). Quantification was performed by using the Bio-1D software.

For glycosidase assays, 20 μl of cell lysates were mixed with 1 μl of either peptide-N-glycosidase F (PNGase F) or endoglycosidase H (Endo H) (Biolabs), and 3 μL of 10× glycoprotein denaturing buffer (Biolabs) prior to incubation at 37 °C for 3 h.

2.4. Indirect immunofluorescence microscopy

A72 and CrFK were transfected with expression plasmids of the different gp3 proteins. At 24 h post-transfection, cells were washed with PBS and fixed with 4% paraformaldehyde in PBS-4% sucrose (Life Technologies). After two washes in PBS, a solution of 50 mM NH$_4$Cl was added for 10 min at room temperature, then fixed cells were incubated with PBS-0.5% bovine serum albumin (BSA) for 30 min. After one wash with PBS-1% BSA and two washes with PBS-1% BSA-0.5% saponine, a mix of primary antibody raised against the Flag tag (Sigma–Aldrich) and either antibody specific of the calnexin (Sigma–Aldrich) or the giantin (Abcam) at dilution of 1/500 in PBS–BSA–saponine solution was added for 1 h at room temperature. For triple labelling in infected cells, a serum of CoV infected cat at a dilution of 1/250 was added to the mix of anti-Flag and anti-calnexin antibodies. After three washes, cells were incubated with a mix of anti-mouse Alexa 488 and anti-rabbit Alexa 555 secondary antibodies (Invitrogen) at working dilutions of 1/600 in PBS–BSA–saponine solution for 45 min at room temperature. For triple staining, secondary antibodies used were anti-cat Alexa 488 (Jackson), anti-mouse Alexa 555 and anti-rabbit Alexa 647 (Invitrogen), all at working dilutions of 1/500. After three washes with PBS, cells were covered with a solution of Mowiol mixed with DAPI for staining of the nucleus. Slides were examined at 63× magnification by apotome microscope (Zeiss) and images were analysed using the Zen software.

2.5. Infections

For infection assays, subconfluent A72 cells were inoculated with type II strain CCoV-1-71, from the American Type Culture Collection (ATCC®VR-809™), at a multiplicity of infection (MOI) of 10. Cells were then incubated for 120 min at 37 °C, with gentle
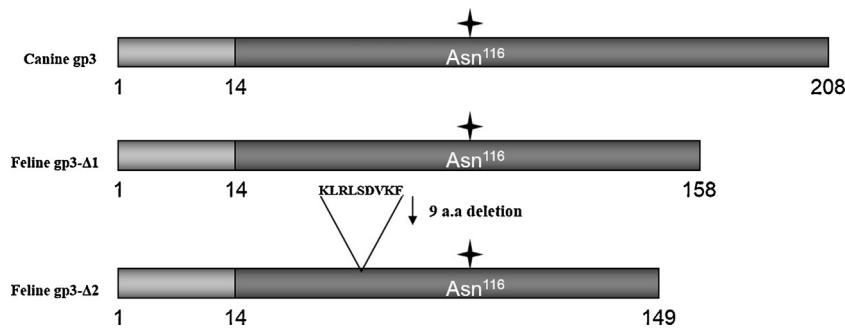
Fig. 1. Schematic representation of the different gp3 proteins. Gp3 is the full length protein encoded by CCoV-I, gp3-Δ1 and gp3-Δ2 arise from atypical FCoV and are deleted of the C-terminus part in comparison with gp3. A deletion of nine amino acids differs between gp3-Δ1 and gp3-Δ2. The potential signal peptide and N-glycosylation site are indicated by a light grey box and a star, respectively. Length of the different proteins is indicated by the number of amino acids at the C-terminus.

rocking for optimal viral adsorption. Inoculum was then replaced by standard fresh medium, supplemented with 10% FBS. Cells were left to incubate for specified amount of time. In parallel, infection of non-transfected cells using the same protocol was conducted.

2.6. Quantitative RT-PCR

Viral RNA was extracted from supernatants using the QIAamp Viral RNA Mini kit (QIAGEN). RNA was reverse transcribed and amplicons were generated using the Quantitect SYBR Green RT-PCR kit (QIAGEN) and the following primers set: CCoV-7F: 5′-GGCAACCCGATGTTTAAAACTGG-3′ and CCoV-7R: 5′-CACTAGATCCAGACGTTAGCTC-3′, following the manufacturer's instructions at an annealing step of 52 °C. These primers target the accessory gene 7b of type II CCoV. Quantification of viral production in cells supernatant was normalised by the total amount of RNA. In cellular extracts, quantitative RT-PCR of the actin housekeeping gene was performed in parallel using the following primers set: ACTIN-F: 5′-CAGCACAATGAAGATCAAGATCATC-3′ and ACTIN-R: 5′-CGGACTCATCGTACTCCTGCTT-3′. The viral RNA copy number in cell extracts was normalised to the expression of the actin gene using the $2\Delta Ct$ method (Livak and Schmittgen, 2001).

3. Results

3.1. Expression of gp3, gp3-Δ1 and gp3-Δ2 in A72 and CrFK cells

The ORF3 genes were cloned into expression plasmids under the control of the CMV promoter with a 3x-Flag tag fused in frame at the 3′ end of ORF3 (Fig. 1). Each plasmid was transfected either in A72 canine cells or in CrFK feline cells. Both cell lines were chosen for their susceptibility to CCoV-II and FCoV-II infections. At 24 h post-transfection, cells were lysed and proteins were detected by immunoblotting with an anti-Flag antibody.

In A72 cells, all three proteins, gp3, gp3-Δ1 and gp3-Δ2 are detected. They migrated according to their predicted molecular weight at 28, 22 and 21 kDa, respectively (Fig. 2A). In CrFK cells, expression of gp3 and gp3-Δ2 was low, whereas gp3-Δ1 was still detected (Fig. 2A). Quantification demonstrates that expression of the gp3-Δ1 is about fivefold higher than gp3 and tenfold more than gp3-Δ2 (Fig. 2B). In A72 cells, differences of expression levels between the three proteins are less pronounced. Quantity of gp3-Δ1 is only twofold more elevated than gp3 and gp3-Δ2.

As gp3 possesses six cysteine residues while gp3-Δ1 and gp3-Δ2 contain only four, we investigated the possible formation of covalent homo-oligomers. At 24 h post-transfection, cell lysates were treated and migrated onto SDS-PAGE gels with or without β-mercaptoethanol. Under non-reducing conditions, supra forms of approximately twice the molecular weight of each protein were

detected. After treatment with β-mercaptoethanol, the monomeric forms were mainly observed, suggesting the assembly of gp3, gp3-Δ1 and gp3-Δ2 into dimeric complexes through disulfide bonds (Fig. 2C). For gp3-Δ1, higher order assemblies were observed, which could correspond to tetramers.

3.2. Post-translational maturation of the proteins

The gp3 proteins bear a putative glycosylation site at the Asn^{116} position. This amino acid is conserved in all three proteins. In order to characterise the glycan, assays with glycosidases were performed. At 24 h post-transfection, cell lysates were incubated either with PNGase F or Endo H or mock treated. PNGase F removes all N-linked glycans whereas Endo H cleaves only polymannose carbohydrates that have not been further processed into complex sugar. Gp3, gp3-Δ1 and gp3-Δ2 are all sensitive to PNGase F (data not shown) and to Endo H (Fig. 3A). These results show that the different gp3 proteins are glycosylated with a high mannose glycan. The same results were obtained in both A72 and CrFK cell lines (data not shown).

In silico analyses indicated an N-terminal hydrophobic domain functioning as signal sequence cleavable after the alanine amino acid in position 15. To test whether this peptide signal is cleaved, mutants without the predicted signal peptide for each protein (ΔSP-gp3, ΔSP-gp3-Δ1, ΔSP-gp3-Δ2) were constructed. Mutants with the cleavage site replaced by five Leucine residues (5L-gp3, 5L-gp3-Δ1, 5L-gp3-Δ2) were also constructed in order to impair the potential cleavage of the signal peptide. At 24 h after transfection, cells lysates were collected, treated or not with Endo H and analysed by immunoblotting. All ΔSP proteins migrated faster than the wild type proteins (Fig. 3B). The estimate apparent molecular weight of the ΔSP proteins was about 3 kDa less than the native proteins. Without a signal peptide, proteins cannot enter the ER and therefore cannot become glycosylated, as confirmed by the same electrophoretic profile of ΔSP proteins treated or not by Endo H. 5L gp3-Δ1 and gp3-Δ2 proteins which harbour an uncleavable signal peptide display a slower migration and an apparent molecular weight of approximately 3 kDa higher than the wild type proteins. Some unglycosylated forms are detected as shown by comparison with lysates treated with Endo H. 5L-gp3 migrated faster than the wild-type protein.

3.3. Subcellular localisation of the proteins

Next, the subcellular localisation of the proteins was examined by colocalisation assays of gp3 proteins with different markers of the cellular compartments in both A72 and CrFK. 24 h post-transfection, dual labelling were carried out with anti-Flag antibody to visualise the gp3 proteins and specific antibodies directed
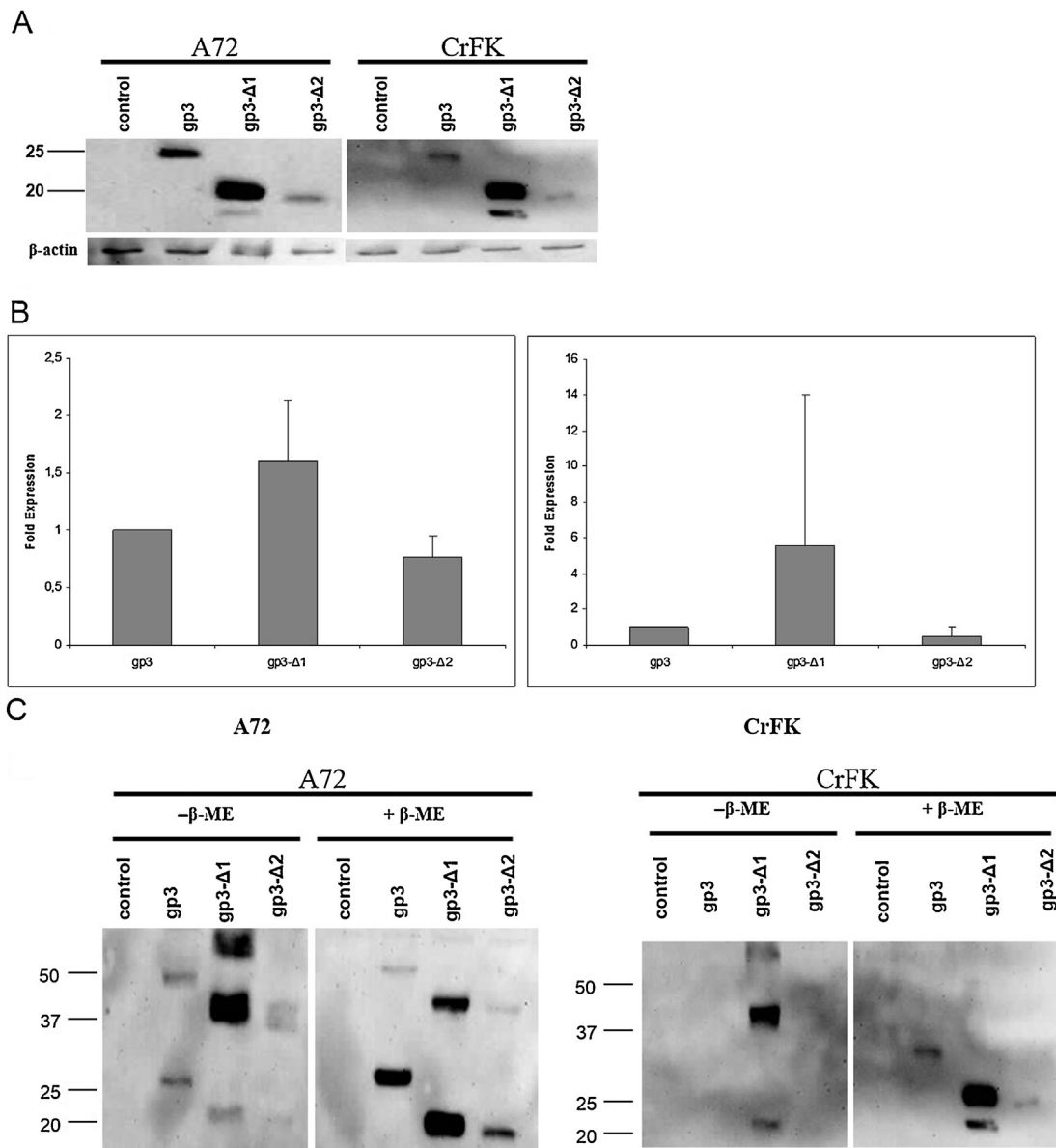
Fig. 2. Protein expression in canine and feline cell types. (A) Detection of the proteins in transfected canine A72 and feline CrFK cells by immunoblotting assays. Cells were transfected with the different gp3 expression plasmids or with an empty pCDNA vector (Control). At 24 h post-transfection, cells were lysed and processed onto SDS-PAGE gels for immunoblotting. Gp3 proteins were detected using an anti-Flag antibody. Cellular β-actin was revealed in parallel by a specific monoclonal anti-actin antibody. (B) Levels of expression of the different gp3 proteins. Immunoblots of the different gp3 proteins were quantified using the Bio-1D software. Quantity of gp3 was arbitrary set to 1 and the relative quantity of gp3-Δ1 and gp3-Δ2 are expressed in comparison with gp3. All data are representative of three independent experiments. Error bars represent standard deviations. (C) Multimerisation of the gp3 proteins. A72 and CrFK cells were transfected with the empty vector pCDNA (control) or plasmids encoding the different gp3 proteins and lysed at 24 h post-transfection. Cell lysates were treated with (+) or without (−) β-Mercaptoethanol (β-ME), prior to migration onto SDS-PAGE gels. Proteins were detected by immunoblotting with anti-Flag antibody. Positions and masses (in kDa) of the molecular mass protein markers are indicated on the left.

against calnexin, a resident protein of the ER, or giantin, a marker of the Golgi apparatus. By apotome microscopy analyses, the fluorescence signals of the gp3 proteins and the giantin were distinct in both A72 and CrFK, indicating that the proteins had not reached the Golgi apparatus (data not shown). In contrast, the gp3 proteins colocalised with calnexin signals in canine and feline cell lines (Fig. 4A and B).

Subcellular localisation of the proteins in a viral context was investigated. A72 cells were infected with the CCoV-II strain at MOI of 10 and transfected 20 h post-infection, with either the empty vector pCDNA3.1 or with plasmids encoding the different gp3 proteins. Cells were then fixed 72 h post-infection and processed for subcellular studies. The fluorescence signals of the

gp3 proteins colocalised with the calnexin signal in infected cells (Fig. 4C).

3.4. CCoV-II viral production in cells expressing the different gp3 proteins

To evaluate the impact of the different gp3 proteins during the viral life cycle, 12 h after transfection with the empty pCDNA3.1 plasmid or plasmids encoding gp3, gp3-Δ1, or gp3-Δ2, A72 cells were infected with CCoV-II strain at MOI of 10. A72 cells were also infected at the same MOI without prior transfection. At 24 h, 48 h and 72 h post-infection, supernatants and cells were collected and analysed by quantitative RT-PCR. Quantity of viral copy
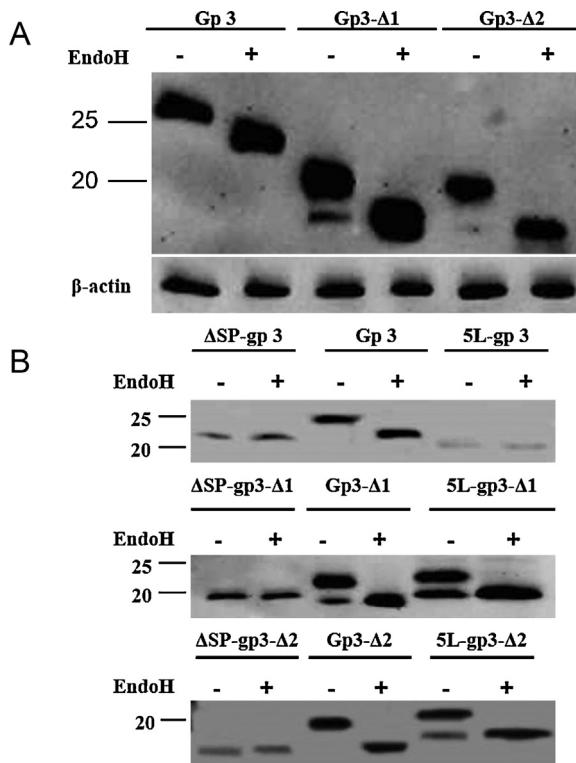
Fig. 3. Processing of the gp3 proteins. (A) Maturation of the N-linked oligosaccharides. A72 cells were transfected with plasmids containing the indicated sequences and lysed at 24 h post-transfection. 20 μL of whole cell lysates were then treated (+) with Endo H or mock treated (−). After migration on SDS-PAGE gels, gp3 proteins were revealed by immunoblotting with the anti-Flag antibody. (B) Cleavage of the signal peptide of the gp3 proteins. A72 cells were transfected with expression plasmids containing different constructs of the gp3 proteins. ΔSP-gp3, ΔSP-gp3-Δ1 and ΔSP-gp3-Δ2 are deleted of the first 14 N-terminal amino acids. In 5L-gp3, 5L-gp3-Δ1 and 5L-gp3-Δ2 constructs, the putative cleavage site was replaced by five Leucine residues, to prevent signal peptide cleavage. At 24 h post-transfection, cell lysates were recovered and treated with (+) or without (−) Endo H treatment, prior to migration. The different proteins were detected by immunoblotting with an anti-Flag antibody. Positions and masses (in kDa) of the protein markers are indicated on the left.

genome in cells supernatant (Fig. 5A) and cellular extracts (Fig. 5B) was calculated and normalised to total RNA amount and the actin housekeeping gene, respectively. No difference was observed between infected cells and infected cells expressing the different gp3 proteins.

4. Discussion

The presence of an additional accessory gene, ORF3 is specific to CCoV-I. In CCoV-II and FCoV-II, only very short sequences, less than 71-nt and corresponding to ORF3, are present and were interpreted by Lorusso et al. (2008) as residual sequences from a CoV ancestor. In FCoV-I, no nucleotide corresponding to ORF3 has been described until our recent study, in which the ORF3 gene was identified in atypical feline CoV strains harbouring an N gene related to CCoV-I and an S gene close to FCoV-I (Le Poder et al., 2013). In these atypical feline strains, the ORF3s are 595-nt or 568-nt in length and are preceded by specific transcription-regulating sequences, suggesting the possible translation into functional proteins during infections.

All ORF3 sequences recovered in these feline CoV strains were deleted the same way, leading either to a putative gp3-Δ1 protein, comprising the first 158 a.a. of gp3 or to gp3-Δ2 protein, with an additional 9 a.a. deletion compared to gp3-Δ1 (Fig. 1). A previous study explored the biochemical properties of the complete canine
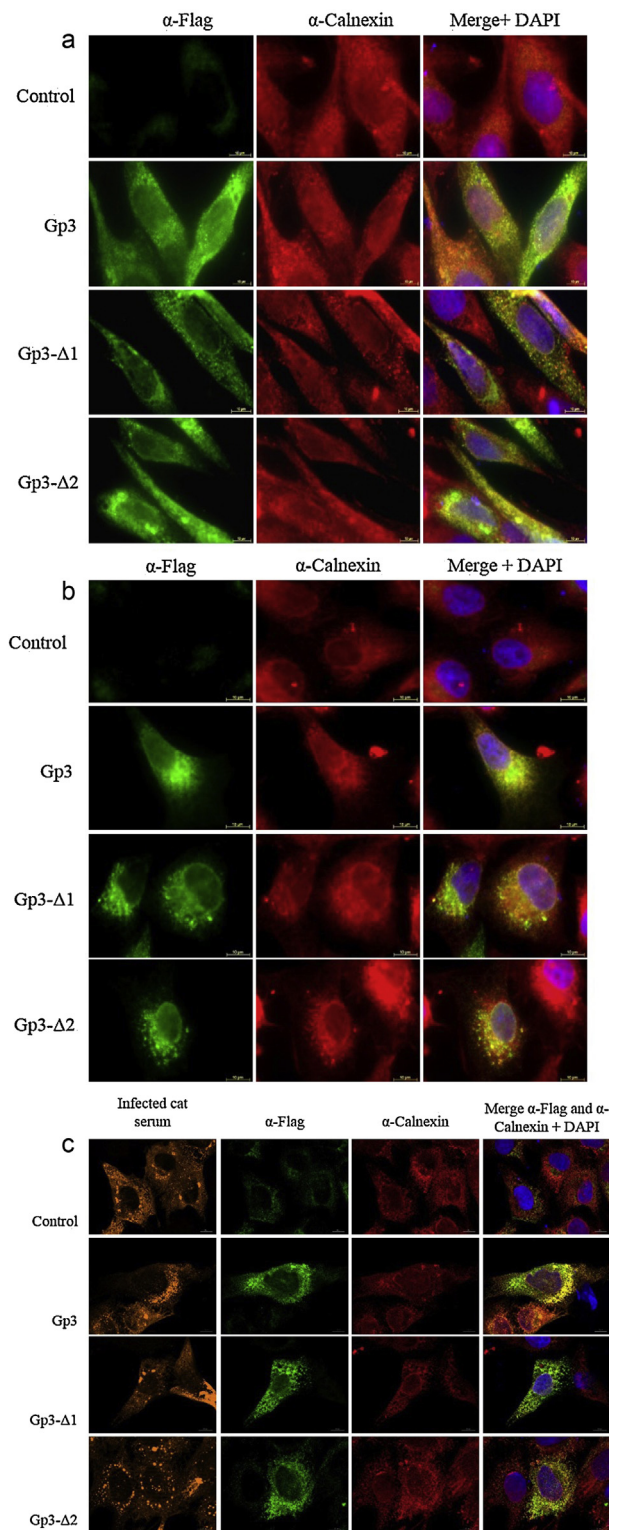

Fig. 4. Subcellular localisation of gp3, gp3-Δ1 and gp3-Δ2. A72 cells (A) and CrFK cells (B) were transfected with an empty pCDNA plasmid (control) or plasmids encoding the different gp3 proteins. At 24 h post-transfection, cells were dual labelled with antibodies against the Flag tag (α-Flag) and against calnexin (α-calnexin), a marker of the ER. Alexa-488 anti-mouse and alexa-555 anti-rabbit were used as secondary antibodies. (C) A72 cells were infected with the CCoV-II 1-71 strain and transfected 20 h post-infection with plasmids containing the indicated sequences. At 72 h post-infection, cells were fixed and triple stained with anti-Flag, anti-calnexin and an anti-CoV serum originating from an infected cat. Cell nuclei were counterstained with DAPI. All slides were observed with a 63× oil immersion objective lens by an apotome microscope (Zeiss). At the right, a merged image of the anti-Flag, the anti-calnexin and the DAPI signal is shown. Bar chart: 10 μm.

gp3 protein using an *in vitro* translation system and concluded that gp3 is a probably secreted, soluble glycoprotein of 28 kDa (Lorusso et al., 2008). Here, the expression of the different gp3, gp3-Δ1 and gp3-Δ2 proteins was analysed in cell culture. Proteins were expressed either in canine or feline cells in accordance to the host tropism from which they were derived. The level of expression is different not only between the two cell lines used, but also between the different proteins. In canine A72 cells, the three proteins are expressed at approximately the same level, but in feline cells, discrepancies between them are very marked. Expression of gp3-Δ1 is fivefold higher than gp3 and gp3-Δ2 (Fig. 2B). Whether these different expressions levels are due to different degradation processes or modulations at the translation step remain to be explored. Expression levels might be influenced by cellular factors involved in regulating protein translation. Interestingly, the gp3 is expressed in canine cells but faintly detected in feline cells which may correlate with the canine virus origin of gp3.

Beside these discrepancies, the proteins have common biochemical properties. In *in vitro* translation assay, gp3 was expressed in a monomeric form (Lorusso et al., 2008). Here, in cell culture, we demonstrated that gp3, but also gp3-Δ1 and gp3-Δ2 oligomerise in, at least, covalent homo-dimers and probably in higher multimeric forms, as shown for gp3-Δ1 (Fig. 2C). The absence of detection of higher multimeric form other than dimers for gp3 and gp3-Δ2 could be due to their fainter expression. The oligomerisation

status of CoV accessory proteins has been investigated for some of them. Multimerization has also been demonstrated for the accessory ORF3 from PEDV (Wang et al., 2012), ORF4a from HCoV-229E (Zhang et al., 2014) or ORF8ab from SARS-CoV (Oostra et al., 2007).

Post-translational modifications are also common to the three proteins in the studied cell lines. *In vitro* translation indicated that gp3 contains an N-linked glycosylation site (Lorusso et al., 2008). In cell culture and through the use of different deglycosidases, we were able to identify the glycan residue as a high polymannose (Fig. 3A), which corroborates with their localisation in the ER (Fig. 4A and B). Indeed, maturation into complex sugar needs processing by enzymes from the Golgi apparatus and presence of a polymannose is characteristic of proteins residing in the ER. It is still unclear how the gp3 proteins are maintained in the ER, as no peculiar signal for ER retention has been identified (Gao et al., 2014). Retention of the gp3 proteins in the ER could have been explained by a non-cleavage of the signal peptide. This hypothesis was tested by molecular mass comparison between native gp3 proteins and proteins either deleted off the signal peptide or harbouring a non-cleavable signal peptide (Fig. 3B). The migration difference between 5L mutants and native proteins strongly suggest an efficient cleavage of the signal peptide in native gp3 proteins. Indeed, 5L-gp3-Δ1 and 5L-gp3-Δ2 have a molecular mass higher than the native gp3-Δ1 and gp3-Δ2. The 5L-gp3 mutant migrated at a lower molecular mass than the native gp3. Lorusso et al. (2008) had already observed
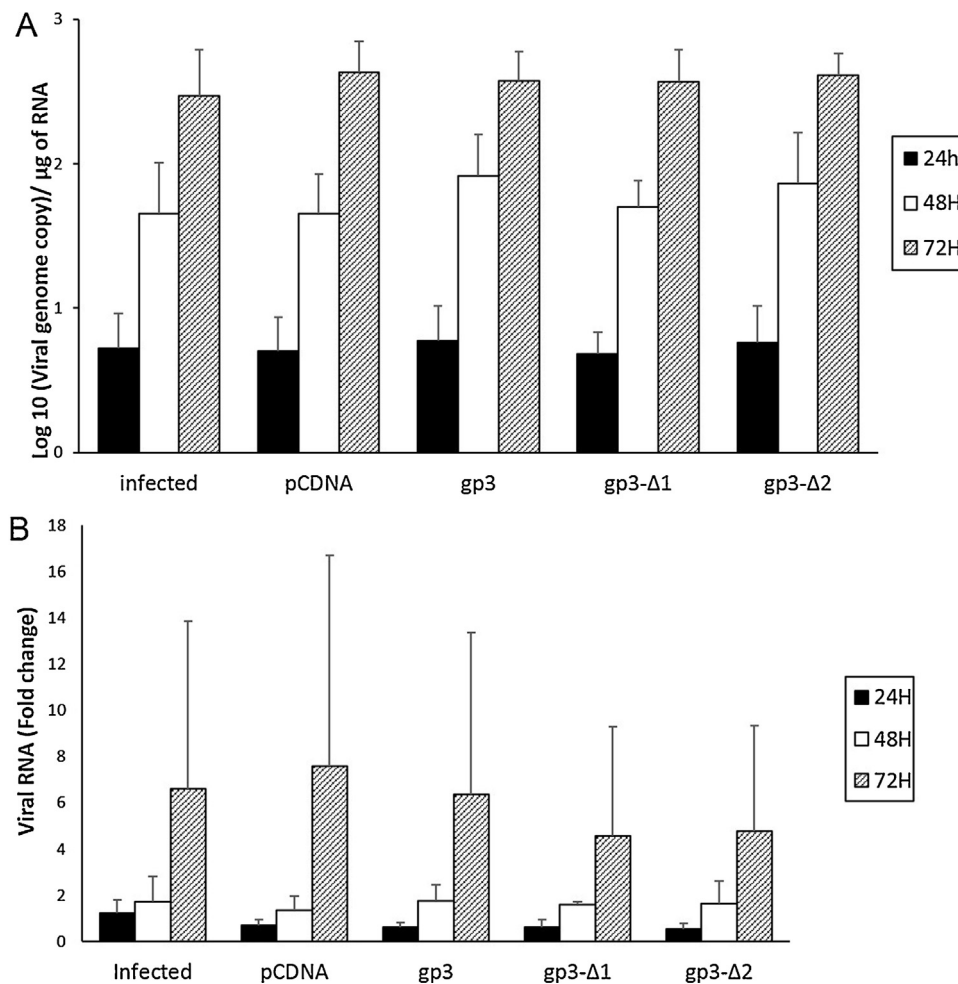

Fig. 5. Viral production of CCoV-II in A72 cells expressing gp3 proteins. A72 cells were transfected with plasmids containing the indicated sequences and infected 12 h post-transfection with the CCoV-II 1-71 strain. Supernatant (A) and cellular extract (B) were collected at 24 h, 48 h and 72 h post-infection and processed for viral genome quantification by quantitative RT-PCR. In supernatants, quantity of viral RNA was normalised by the total amount of RNA. Mean expression of intracellular viral RNA copy numbers normalised to actin are given, using the 2ΔCt method. Means from triplicate experiments are given. Error bars represent standard deviations.

that the presence of the signal peptide in gp3 induced an aberrant faster migration similar to our observation herein. Thus, retention in the ER of the gp3 proteins is not due to a default in the signal peptide cleavage. To investigate whether viral proteins may influence the subcellular localisation of gp3 proteins, A72 were infected with a CCoV-II strain, which does not express gp3, then transfected with plasmids encoding the different gp3. Again in this viral context, gp3 proteins are localised in the ER (Fig. 4C). Altogether, these results strongly suggest that the gp3 proteins could be maintained in the ER through interactions with cellular factors, as proposed by studies on the ORF8ab protein of the SARS-CoV (Oostra et al., 2007).

From the comparative study of the complete gp3 and the deleted mutant gp3-Δ1 and Δ2, we can deduce that the first 158 amino acids contain the necessary signals for the basic features of the proteins: the cysteine residues for oligomerisation, the N-glycosylation site and the unknown retention determinant in the ER. These conserved properties might be important for their function.

In the absence of laboratory strains harbouring ORF3 gene, i.e. CCoV-I strains or the atypical FCoV strains, the only way to study the different gp3 proteins in virus infected cells was to infect transfected cells with a CoV strain that does not encode gp3. As the gp3 proteins are better expressed in canine A72 cells than in feline CrFK cells, the impact of gp3 on viral replication efficiency was investigated in transfected A72 infected by a CCoV-II virus. In this context, the viral production is similar in cells expressing gp3 in comparison with the empty plasmid transfected cells or only infected cells (Fig. 5). As gp3 is present only in CCoV-I strain and deleted gp3 in some atypical FCoV strains, it is plausible that the function of these proteins is crucial only for these particular CCoV and FCoV and thus could not be observed in the model developed herein. However, most accessory proteins have no effect on viral life cycle in in vitro assays (Hodgson et al., 2006; Haijema et al., 2004), except those acting as viroporins like ORF3 of PEDV (Wang et al., 2012), ORF3a of SARS-CoV (Chan et al., 2009) and ORF4a of HCOV-229E (Zhang et al., 2014). Nevertheless, their persistence in the viral genome suggests their biological importance in vivo. Yet, recent studies proved that accessory proteins might have a wide range of functions including modulation of viral pathogenicity like ORF7 of TGEV, which absence increases cell RNA degradation and viral pathogenicity in infected piglets (Cruz et al., 2011). Others act as counteragents of the innate immunity like ORF7a of FCoV or ORF6 of SARS-CoV to name a few (Dedeurwaerder et al., 2014; Frieman et al., 2007). Some others are crucial in viral tropism. As an example, ORF3c of FCoV is necessary for the confinement of the feline virus in the intestinal tract, whereas FCoV without this gene disperses through viraemia in the feline host (Bálint et al., 2014). During host change, mutations of accessory proteins have also been observed, suggesting a possible role in adaptation of CoV to their host. Thus, during the adaptation of CCoV-II to swine, leading to the emergence of TGEV, deletion of ORF7b and ORF3b occurred (Decaro et al., 2007). In the same manner, whereas SARS-CoV strains infecting bats and civets harbour an intact ORF8ab gene, a 29-nt deletion is systematically observed in strains infecting humans, leading to the translation of two novel proteins 8a and 8b (Guan et al., 2003). Gp3 has many common features with ORF8ab. Both accessory proteins oligomerise through disulfide bonds and are maintained in the ER without any specific retention signal. The ER is a crucial cellular compartment for folding and maturation of novel synthesised proteins. ORF8ab has been demonstrated to facilitate protein folding by up-regulating the activating transcription factor 6 (ATF6) (Sung et al., 2009). Whether gp3 could also facilitate viral protein synthesis needs to be further investigated, by studying its impact on the ER protein translation and regulation activities. Deletions in ORF8ab lead to two new putative proteins ORF8a and ORF8b which are unstable in mammalian cells and with different subcellular localisation compared to ORF8ab. In contrast, deleted forms

of gp3 conserve the same basic features and could have a similar function than intact gp3.

In concordance with other studies, our data underline the importance to investigate the role of CoV accessory proteins during the viral adaptation to new hosts. In the context of emergence of high virulent CoVs such as SARS-CoV or MERS-CoV arising from animals, it remains important to understand the mechanisms of CoV pathogenicity and cross-species transmissions.

References

Bálint, Á., Farsang, A., Zádori, Z., Belák, S., 2014. Comparative in vivo analysis of recombinant type II feline coronaviruses with truncated and completed ORF3 region. PLOS ONE 9, e88758.
Bredenbeek, P.J., Pachuk, C.J., Noten, A.F., Charité, J., Luytjes, W., Weiss, S.R., Spaan, W.J., 1990. The primary structure and expression of the second open reading frame of the polymerase gene of the coronavirus MHV-A59; a highly conserved polymerase is expressed by an efficient ribosomal frameshifting mechanism. Nucleic Acids Res. 18, 1825–1832.
Chan, C.-M., Tsoi, H., Chan, W.-M., Zhai, S., Wong, C.-O., Yao, X., Chan, W.-Y., Tsui, S.K.-W., Chan, H.Y.E., 2009. The ion channel activity of the SARS-coronavirus 3a protein is linked to its pro-apoptotic function. Int. J. Biochem. Cell Biol. 41, 2232–2239.
Cruz, J.L.G., Sola, I., Becares, M., Alberca, B., Plana, J., Enjuanes, L., Zuñiga, S., 2011. Coronavirus gene 7 counteracts host defenses and modulates virus virulence. PLoS Pathog. 7, e1002090.
Decaro, N., Buonavoglia, C., 2008. An update on canine coronaviruses: viral evolution and pathobiology. Vet. Microbiol. 132, 221–234.
Decaro, N., Martella, V., Elia, G., Campolo, M., Desario, C., Cirone, F., Tempesta, M., Buonavoglia, C., 2007. Molecular characterisation of the virulent canine coronavirus CB/05 strain. Virus Res. 125, 54–60.
Dedeurwaerder, A., Olyslaegers, D.A.J., Desmarets, L.M.B., Roukaerts, I.D.M., Theuns, S., Nauwynck, H.J., 2014. ORF7-encoded accessory protein 7a of feline infectious peritonitis virus as a counteragent against IFN-α-induced antiviral response. J. Gen. Virol. 95, 393–402.
Dijkman, R., Jebbink, M.F., Wilbrink, B., Pyrc, K., Zaaijer, H.L., Minor, P.D., Franklin, S., Berkhout, B., Thiel, V., van der Hoek, L., 2006. Human coronavirus 229E encodes a single ORF4 protein between the spike and the envelope genes. Virol. J. 3, 106.
Frieman, M., Yount, B., Heise, M., Kopecky-Bromberg, S.A., Palese, P., Baric, R.S., 2007. Severe acute respiratory syndrome coronavirus ORF6 antagonizes STAT1 function by sequestering nuclear import factors on the rough endoplasmic reticulum/Golgi membrane. J. Virol. 81, 9812–9824.
Gao, C., Cai, Y., Wang, Y., Kang, B.-H., Aniento, F., Robinson, D.G., Jiang, L., 2014. Retention mechanisms for ER and Golgi membrane proteins. Trends Plant Sci. 19, 508–515.
Gorbalenya, A.E., Enjuanes, L., Ziebuhr, J., Snijder, E.J., 2006. Nidovirales: evolving the largest RNA virus genome. Virus Res. 117, 17–37.
De Groot, R.J., 2006. Structure, function and evolution of the hemagglutinin–esterase proteins of corona- and toroviruses. Glycoconj. J. 23, 59–72.
Guan, Y., Zheng, B.J., He, Y.Q., Liu, X.L., Zhuang, Z.X., Cheung, C.L., Luo, S.W., Li, P.H., Zhang, L.J., Guan, Y.J., et al., 2003. Isolation and characterization of viruses related to the SARS coronavirus from animals in southern China. Science 302, 276–278.
Haijema, B.J., Volders, H., Rottier, P.J.M., 2004. Live, attenuated coronavirus vaccines through the directed deletion of group-specific genes provide protection against feline infectious peritonitis. J. Virol. 78, 3863–3871.
Hodgson, T., Britton, P., Cavanagh, D., 2006. Neither the RNA nor the proteins of open reading frames 3a and 3b of the coronavirus infectious bronchitis virus are essential for replication. J. Virol. 80, 296–305.
Livak, K.J., Schmittgen, T.D., 2001. Analysis of relative gene expression data using real-time quantitative PCR and the 2(−delta delta C(T)) method. Methods (San Diego, Calif.) 25, 402–408.

Lorusso, A., Decaro, N., Schellen, P., Rottier, P.J.M., Buonavoglia, C., Haijema, B.-J., de Groot, R.J., 2008. Gain, preservation, and loss of a group 1a coronavirus accessory glycoprotein. J. Virol. 82, 10312–10317.

McBride, R., Fielding, B.C., 2012. The role of severe acute respiratory syndrome (SARS)-coronavirus accessory proteins in virus pathogenesis. Viruses 4, 2902–2923.

Oostra, M., de Haan, C.A.M., Rottier, P.J.M., 2007. The 29-nucleotide deletion present in human but not in animal severe acute respiratory syndrome coronaviruses disrupts the functional expression of open reading frame 8. J. Virol. 81, 13876–13888.

Pedersen, N.C., 2009. A review of feline infectious peritonitis virus infection: 1963–2008. J. Feline Med. Surg. 11, 225–258.

Le Poder, S., Pham-Hung d'Alexandry d'Orangiani, A.-L., Duarte, L., Fournier, A., Horhogea, C., Pinhas, C., Vabret, A., Eloit, M., 2013. Infection of cats with atypical feline coronaviruses harbouring a truncated form of the canine type I nonstructural ORF3 gene. Infect. Genet. Evol. 20, 488–494.

Sung, S.-C., Chao, C.-Y., Jeng, K.-S., Yang, J.-Y., Lai, M.M.C., 2009. The 8ab protein of SARS-CoV is a luminal ER membrane-associated protein and induces the activation of ATF6. Virology 387, 402–413.

Wang, K., Lu, W., Chen, J., Xie, S., Shi, H., Hsu, H., Yu, W., Xu, K., Bian, C., Fischer, W.B., et al., 2012. PEDV ORF3 encodes an ion channel protein and regulates virus production. FEBS Lett. 586, 384–391.

Zhang, R., Wang, K., Lv, W., Yu, W., Xie, S., Xu, K., Schwarz, W., Xiong, S., Sun, B., 2014. The ORF4a protein of human coronavirus 229E functions as a viroporin that regulates viral production. Biochim. Biophys. Acta 1838, 1088–1095.